TECHNICAL MEMORANDUMS

NATIONAL ADVISORY COMMITTEE FOR AERONAUTICS

No. 827

HELICOPTER PROBLEMS

By H. G. Küssner

Luftfahrtforschung
Vol. 14, No. 1, January 20, 1937
Verlag von R. Oldenbourg, München und Berlin

Washington
May 1937

NATIONAL ADVISORY COMMITTEE FOR AERONAUTICS

TECHNICAL MEMORANDUM NO. 827

HELICOPTER PROBLEMS*

By H. G. Küssner

The present report deals with a number of the main problems requiring solution in the development of helicopters and concerning the lift, flying performance, stability, and drive.

A complete solution is given for the stability of the helicopter with rigid blades and control surfaces. With a view to making a direct-lift propeller sufficient without the addition of auxiliary propellers, the "flapping drive" is assessed and its efficiency calculated.

I. INTRODUCTION

The idea of the helicopter is as old as aviation itself. Leonardo da Vinci designed a helicopter, but the first air-borne models did not appear until the 19th century, and the development of the airplane at the beginning of the 20th century ran parallel with the helicopter until the former gradually pushed the latter into the background. The first man-carrying helicopters were never able to pass beyond the stage of air jumps at best, since they were unstable in flight and mechanically extremely sensitive. But now that sufficient experience in light design and in aerodynamics is available, the prospects of helicopter development are much more promising; and this is in no small measure due to de la Cierva's pioneering labor. A notable historical outline of helicopter development is found in Lamé's book (reference 1).

The autogiro is the first successful aircraft on which the momentum for overcoming the gravity is produced by the downwash of an airfoil system which, apart from the translatory motion, executes an additional rotatory motion about a fixed body axis.

---

*"Probleme des Hubschraubers." Luftfahrtforschung, vol. 14, no. 1, January 20, 1937, pp. 1-13.

The autogiro has solved the problem of horizontal flight of helicopters up to such a low speed that one is even tempted to forego the floating power at $v = 0$, since the frequently prevailing wind velocity still enables the autogiro to hover over a certain point and to land as well. Besides, a real helicopter should be capable of rising and landing with horizontal speed in gusty weather. Lastly, de la Cierva developed the jump-start method which allows the forcing of the autogiro several meters straight up in the air - which, properly handled, suffices for reaching stalling speed without a second ground contact (reference 2). So the autogiro has come quite close to the performances which originally had been commonly accepted as being reserved for the helicopter alone. On the other hand, it also has its limitations both as to application and to drawbacks. The comparatively small climbing angle makes a free space necessary for the take-off. The handling in side wind is difficult, and so is the stalled landing. At high flying speed the longitudinal control is very sensitive. Besides, the rotor may get out of step.

Thus, one logical trend in development would be to give the autogiro the still lacking helicopter properties: vertical stationary ascent and descent, and hovering without, however, depriving it of any of its developed good characteristics. Several new, successful helicopter designs are along these lines. Right now the helicopter is best situated for catching up with the technical advantages of the airplane and for opening up new possibilities of use through its unique floating power.

Just as the airplane enjoys its present state of development as a result of the intensive theoretical and experimental exploration of all problems arising with the airplane, so the further development of the helicopter is in need of clearness regarding the typical helicopter problems which are unknown to the airplane.

The following arguments are a contribution in particular to the elucidation of the problems of stability and of the power of the lifting propeller in sustained flight (hovering). Further, the creation of lifting force and the expected flight performances are treated in light of the present state of research.

II. NOTATION

a	(m)	radius of propeller disk.
A	(kg)	motive ~~power~~ force
B		amplitude of rotation of blade.
c	(m/s)	velocity of flow.
F	(m^2)	control surface.
$F_s=\pi a^2$	(m^2)	propeller disk area.
F_w	(m^2)	equivalent flat-plate area.
F_{w_s}	(m^2)	equivalent flat-plate area of propeller blade.
G	(kg)	gross weight.
h	(m)	1) distance of c.g. from the plane of the propeller disk, 2) coefficient of power loss.
H	(m kg/s)	power loss.
J	(m kg s)	~~free helical motion~~ angular momentum of the rotor.
K_a	(kg)	thrust.
l	(m)	semiwing chord.
L	(m kg/s)	power input.
M	(m kg)	moment (torque)
m	(kg s^2/m)	1) mass of the helicopter. 2) moment coefficient.
N	(m kg/s)	transmitted effective power.
P_{xz}, P_{yz}	(m kg)	moment of precession.
$r=\sqrt{x^2+z^2}$		1) radius vector. 2) coordinate in propeller radius direction. 3. root of the characteristic equation.

s	(m)	wall distance of the propeller disk area.
$u=\omega a$	(m/s)	tip speed.
v	(m/s)	flying speed.
v_z	(m/s)	rate of climb.
w	(m/s)	axial velocity.
W	(kg)	drag.
x, y, z		coordinates.
α, β		angle between the z-axis and the thrust axis projected on planes xz and xy.
γ		1) criterion for rolling moment. 2) flapping angle.
ϵ		lift-drag ratio.
ζ		coefficient of propeller reactions.
ϑ		1) angle between the z-axis and the radius vector. 2) anfle of antirotation.
$h\theta$	(m kg/s^2)	mass moment of inertia of the helicopter with respect to the c.g. of the blades.
κ		criterion of helical motion.
$\lambda=c/u$		coefficient of advance.
μ		slipstream contraction factor.
ν	(1/s)	vibration frequency.
ρ	(kg s^2/m^4)	air density.
$\sigma=\sqrt{s/a}$		characteristic of wall distance.
φ		phase angle.
Φ		velocity potential.
ω	(1/s)	angular velocity.

III. CREATION OF LIFTING FORCE

The symmetrical axial ideal flow around a sustained lift propeller was originally treated by H. Kimmel in his thesis of 1912 at Munich (reference 3). Even though his solution had been reached on the basis of various simplifying premises which do not occur in reality, it is nevertheless desirable, when designing a helicopter, to be able to predict, at least roughly, the air motions to be expected - whether to afford a control of their effect on any stabilizing surface or a check on the mutual interference of several rotors. For this reason, a brief summary of Kimmel's results should be of interest.

The symmetrical axial ideal flow on a sustained lifting propeller may be visualized by superposition of several potentials. Let us assume that the axial velocity of flow through the propeller disk area is constant. Disposing vortex sources on the disk area from which the air with the constant axial velocities $\pm\frac{w}{2}$ flows out at both sides, and denoting with $P_n(\cos\vartheta)$ the zonal harmonic spherical functions of the first type, the potential for the propeller disk radius $a = 1$ is, according to Kimmel (fig. 1, left):

$$\left.\begin{aligned} r < 1:\ \Phi_a &= \frac{w}{2}\left[-P_0 + r\,P_1 - \frac{r^2}{2}P_2 \right.\\ &\qquad \left. + \frac{r^4}{2\times4}P_4 - \frac{1\times3\times r^6}{2\times4\times6}P_6 + - \ldots\right]\\ r > 1:\ \Phi_a &= \frac{w}{2}\left[-\frac{1}{2}\frac{P_0}{r} + \frac{1}{2\times4}\frac{P_2}{r^3} \right.\\ &\qquad \left. - \frac{1\times3}{2\times4\times6}\frac{P_4}{r^5} + - \ldots\right] \end{aligned}\right\} \cdots (1)$$

Prescribing a constant axial velocity $+\frac{w}{2}$ through the propeller disk area affords the potential (fig. 1, right-hand side):

$$\left.\begin{aligned} r < 1: \quad \Phi_c &= \frac{w}{\pi}\left[- P_0 + \frac{\pi}{2} r P_1 - r^2 P_2 \right. \\ &\qquad \left. + \frac{r^4}{3} P_4 - \frac{r^6}{5} P_6 + - \ldots \right] \\ r > 1: \quad \Phi_c &= \frac{w}{\pi}\left[- \frac{1}{3}\frac{P_1}{r^2} + \frac{1}{5}\frac{P_3}{r^4} \right. \\ &\qquad \left. - \frac{1}{7}\frac{P_5}{r^6} + - \ldots \right] \end{aligned}\right\} \cdots (2)$$

Superposition of the two potentials Φ_a and Φ_c results in a flow whose axial velocity has, at one side of the propeller disk area, the constant value $\frac{w}{2} + \frac{w}{2} = w$ and at the other side, the value zero.

This flow corresponds to the rotor inflow. For a rough computation of the outflow, we consider the zone B, which is assumed to be bounded by the propeller disk area and the cylindrical surface $r = 1$, and extending to infinity toward the z-axis. We then assume in this zone a stream of constant axial velocity $2w$ having a potential

$$\Phi_b = 2w\, z$$

On forming the potential,

$$\Phi_b - \Phi_a - \Phi_c$$

in the zone B we find on the propeller disk area the constant axial velocity $2w - w = w$, whereas at infinity the axial velocity $2w$ prevails. The slipstream contraction factor is $\mu = \frac{1}{2}$. In addition, there is a constant pressure jump along the entire propeller disk area to the amount of

$$\Delta p = 2\rho\, w^2$$

This assumption is contained in all propeller theories and is evidently valid so long as the axial velocity of flow through the swept disk area remains roughly constant. This is the case for propellers having low pitch and multiple blades; hence, especially appropriate for direct-lift propellers.

At the edge of the plane of passage the streamlines are - theoretically - substantially curved, according to figure 2. Thus, in reality a vortex ring forms around the border line which can be observed occasionally even in torque-stand tests of regular propellers.

If two coaxial propellers are disposed closely over one another, they can be approximately substituted by a propeller disk area. If the distance of the propeller planes is greater, the bottom propeller draws in an additional quantity of air which, by given stream energy, amplifies the impulse. However, the attainable gain is much less than afforded by mounting the two propellers side by side.

The impulse produced by the stream is always followed by a loss of power. Consider a stream with the asymptotic end section F_o and constant stream velocity w_o in this section. The normal force produced by this stream is equal to the impulse per unit time of fluid quantity passing through the jet. That is, it is

$$A = \frac{d}{dt} (m\, w_o) = \rho\, F_o\, w_o^2 \tag{3}$$

The power absorbed to produce the impulse is:

$$N = \frac{dm}{dt} \frac{w_o^2}{2} = \rho\, F_o\, \frac{w_o^3}{2} \tag{4}$$

Eliminating w_o from (3) and (4) leaves:

$$A^3 = 4\, N^2\, \rho\, F_o \tag{5}$$

To compute the power from this (5), we introduce an assumption concerning the asymptotic end cross section F_o of the jet in ideal flow. For in real viscous fluid the jet is in a continuous process of dissolution while forming a mixing zone, so in that case there can be no question about an asymptotic end cross section. In conformity with the above, we introduce for a free cylindrical jet the contraction factor $\mu = \frac{1}{2}$, so that

$$F_o = \mu\, F_s = \tfrac{1}{2}\, F_s \tag{6}$$

We further introduce, for abbreviation, the thrust coefficient and the ~~moment~~ torque coefficient:

$$k_s = \frac{A}{\frac{\rho}{2} u^2 F_s}; \quad k_d = \frac{M}{\frac{\rho}{2} u^2 F_s a} \tag{7}$$

Writing (6) and (7) in (5) gives the Bendemann equation:

$$k_d = \frac{1}{2} k_s^{3/2} \tag{8}$$

It is presumed that the blades are controllable, as in the majority of modern helicopters. For a helicopter with fixed blades is comparable to an airplane which can only fly at a certain angle of attack and is therefore difficult to manage.

Plotting k_s against k_d for a predetermined direct lift propeller affords a set of curves resembling in significance the profile polars of an airplane. The k_d/k_s ratio is a measure for the quality of the rotor and reaches its optimum value at a certain thrust coefficient k_{s_o}, similar to the airplane lift/drag ratio. Bendemann's curve (8), shown ~~in dashes~~ solid in figure 3, has in this representation a significance similar to the induced-drag parabola in profile polar curves. The real helicopter polar is shifted a certain amount to the right to allow for the frictional drag of the blades.

For propellers with low thrust coefficient and small coefficient of advance - that is, for helicopter propellers in particular - the propeller theory can be linearized conformable to airfoil theory. The circulation decrease at the blade tip can be allowed for conformably to the screen-flow theory, as employed by O. Walchner (reference 4) for cylindrical, nontwisted propeller blades and definite blade number to improve Bendemann's equation. The improved parabola is the dashed curve in figure 3. It will be seen that theory and experiment are in agreement up to a profile friction drag, which in itself increases somewhat with the angle of attack.

Bringing a constant-speed helicopter propeller closer to a parallel flat wall results in a different thrust as well as torque. If s is the wall distance, these changes are properly represented as function of the parameter

$$\sigma = \sqrt{\frac{s}{a}}$$

These changes were investigated by the writer with a model propeller of 1 meter diameter which had four blades of optimum twist and a constant chord of 50 millimeters. Its thrust coefficient k_s is shown plotted against σ in figure 4; its moment coefficient k_d in figure 5.

From this it may be deduced that for finite wall distance the moment is smaller or only slightly greater than in unlimited flow because the quantity of fluid passing through it becomes less as the wall is approached. In accord with it, the thrust also decreases with decreasing σ somewhat in the same ratio, at first, as the moment. This decrease is, as proved by the measurements, markedly influenced by the characteristic value. On further decrease of σ the passing fluid quantity decreases still more, so that the moment drops very substantially. The smaller the velocity of discharge, the more the angle of attack of a blade element approaches its angle of inclination relative to the wall, at which the blade circulation and consequently, the thrust is increased. This increase is little dependent on the characteristic value and is almost linear with σ in the range of $\sigma = 0$ to 0.8. In the extreme case $\sigma = 0$, the thrust would be approximately double if the blade chord were sufficiently small. The point $\sigma = 1$ is worthy of notice as the point where all measurements of thrust and moment are approximately the same as in unlimited fluid. For this reason helicopter propeller measurements should be made at ground distances either in excess of 5 times the propeller radius or else about equal to the propeller radius in order to simulate the conditions in free atmosphere.

For $\sigma > 1$ the ground effect is small and hardly alters the k_d/k_s ratio. In the zone of $\sigma < 1$ this ratio drops very considerably and fairly suddenly. At constant power this means a rise in thrust. On landing, this acts like a springy cushion; that is, it reduces the landing shock, provided the propeller can approach the ground closely enough. Otherwise, it may happen that a helicopter with insufficient engine power is able to float on this air cushion without being able to rise any higher. In addition, this air cushion produces a stabilizing moment which tends to bring the propeller disk area parallel with the ground if the distance is $s < a$; that is, $\sigma < 1$.

IV. FLIGHT PERFORMANCES OF THE HELICOPTER

The power loading of the helicopter while being sustained in free air is:

$$\frac{N}{G} = u \frac{k_d}{k_s} \text{ m/s} \qquad (9)$$

On a model lifting propeller, with rectangular nontwisted blades, for example, the following optimum values were obtained:

Number of blades	k_s	k_d/k_s
z = 2	0.005	0.087
z = 4	.008	.109

By very low thrust loading k_s and given tip speed u, the two-blade helicopter propeller is - as regards power required - superior to the four-blade one. But in order to avoid abnormal dimensions, higher k_s values are much preferred. On the other hand, the thrust loading is upwardly limited by the requirement to be able to make a forced glide landing with autorotating propeller in case of engine failure - a stipulation so very natural and justified that it already serves as the correct method in helicopter development. Actually built helicopters of this kind, with three to four blades tapered toward the tip, have:

$$k_s \sim 0.013 \text{ to } 0.015; \quad k_d/k_s \sim 0.09$$

Admittedly, helicopters with $k_s = 0.032$ have also been built, but for special reasons which are associated with stabilization. Then the k_d/k_s ratio probably amounts to at least 0.12. The autorotation of such highly loaded propellers with comparatively high pitch, causes difficulties, especially if coaxially arranged. But, aside from all that, the rate of descent in an emergency landing would be inadmissibly high.

To invoke a comparison, it may be added that for an autorotating propeller in horizontal flight, the thrust coefficient referred to tip speed amounts to $k_s \sim 0.015$ and that the best horizontal ϵ is:

$$\epsilon_{min} \sim 0.11 \quad \text{for} \quad \lambda \sim 0.4 \text{ to } 0.5$$

The position of the optimum tip speed decisive for the power required of helicopters, must be defined by complete mathematical analysis of comparative designs. The greater the taper of the blades, the higher the optimum of u will be. As a rule, values of $u < 100$ m/s lead to uneconomical enlargement of the size of the propellers; hence modern helicopters fly like the autogiro with

$$u \sim 110 \text{ to } 130 \text{ m/s}$$

Writing these values into (9) gives an average of $\frac{N}{G} = 11$ m/s.

The regulations of the DLA stipulate that every airplane at take-off must have an excess power so that its rate of climb is $w \geq 2.5$ m/s. This readily suggested utilizing this minimum for the vertical take-off of a helicopter as well. An average ranges around

$$\frac{N}{G} = 11 + 2.5 = 13.5 \text{ m/s}$$

$$75 \frac{G}{N} = 5.55 \text{ kg/hp.}$$

This power loading is reached by the latest helicopters - although seldom - it usually falling a little lower. The constructional difficulties are at present still too great to assure a helicopter with much lower power loading capable, with its excess power, of developing a high speed of climb.

According to a previous statement, the jet velocity of the helicopter in ideal flow is at infinity $w_o = 2w$ where w is the rate of flow through the propeller disk area. Then, according to (3) the lift is

$$A = \frac{dm}{dt} 2w \qquad (10)$$

The air mass per second sharing in the impulse creation is, in the case of the helicopter, the product of propeller disk area πa^2, the rate of flow w, and the air density ρ. In the case of the airplane wing with small angle of attack, it leads to an equation similar to (10), with w denoting the vertical velocity at the place of

the wing, and $2w$ the velocity far downstream from it. The air mass per second contributing to the impulse creation of wings with elliptical span-load distribution and span b is the product of section $\pi b^2/4$ of a tube of flow, the rate of flow c through this section, and the air density.

Visualizing the propeller disk area of the helicopter propeller as wing area, the section of the tube of flow is:

$$F = \pi \frac{(2a)^2}{4} = \pi a^2$$

that is, again equal to the propeller disk area. This interpretation has proved itself in the theory of the autorotating propeller with small angle of attack. The appearing flow loss merely serves to cover the friction losses of the wing, but does not reduce the air mass sharing in the impulse creation (cf. reference 4a).

It is very natural now to generalize these two results, which for the moment are valid only for two limiting cases, to include any flow direction of the propeller. We assume that the contributing air mass is always obtained as quantity of flow through a sphere circumscribed about the lifting propeller. Of course, this assumption is only roughly correct, aside from the fact that corrections due to finite blade number must be made. The precise theoretical treatment of this quite difficult problem is still lacking.

This assumption allows the calculation of the power required for impulse creation by any helicopter motion. The impulse always acts against the direction of the absolute velocity with respect to the fluid at rest at infinity. Suppose the direction of the flying speed v of the helicopter inclines toward this direction at an angle ϑ. Then the rate of flow through the circumscribed sphere after vectorial addition of v and w is:

$$c = \sqrt{v^2 - 2v\,w\cos\vartheta + w^2} \qquad (11)$$

We finally obtain as impulse force and power

$$\left.\begin{aligned} A &= \rho F_s c\, 2w \\ N_i &= A\, w \end{aligned}\right\} \qquad (12)$$

For the special case of $\vartheta = 90^\circ$, equations (11) and (12), we obtain the equations already reported by Margoulis (reference 5). Now the two following extreme cases obtained from (12) by eliminating w are important:

$$v \longrightarrow 0: \quad A^3 = 2\rho F_s N_i^2 \tag{13}$$

$$w \longrightarrow 0: \quad A^2 = 2\rho F_s v N_i \tag{14}$$

Equation (13) is identical with Bendemann's equation (8), while (14) contains the known approximation formula for the induced drag of a circular airfoil.

The friction power of a helicopter in arbitrary flow direction is only roughly approximative, because the inside blade elements are occasionally under high angles of attack and are attacked from the trailing edge. For such cases it is hardly possible to give exact friction factors. Besides, even if these values were known, the integration - i.e., the formulation - of a mean friction power value with respect to time, is quite tedious. For that reason, we shall simplify the present problem step by step.

First, we assume the blades to be so formed and controlled that all blade profiles remain within an angle of attack range below burbling. For this range a constant mean value $\overline{c_w}$ of the friction factor for all blade profiles is assumed. If c is, as before, the rate of flow, the relative velocity at the place of any wing element in symmetrical axial stationary flow is:

$$v = (c^2 + r^2 \omega^2)^{1/2}$$

The profile friction produces a frictional moment about the propeller axis as well as a drag of the whole propeller in axial direction. It is a widely spread mistake to assume that the circulation of the blades would have to disappear at zero thrust and that therefore in this operating condition, one could measure the frictional moment of the propeller alone. This erroneous deduction is avoided by a vigorous assumption which contains the rotatory and translatory share of the friction power entire (undivided). The total friction power of the propeller with z blades is:

$$N_R = \rho z \overline{c_w} \int_0^a l(r) v^3 \, dr \tag{15}$$

In the most elementary case of wing chord $2l$ = constant, the friction power with $\lambda = c/u$ becomes:

$$\left.\begin{aligned} N_R &= \rho\, u^3\, z\, l\, a\, \overline{c_w}\, f_1(\lambda) \\ &= \frac{\rho}{2}\, u^3\, F_{w_s}\, f_1(\lambda) \\ f_1(\lambda) &= \left(\frac{1}{4} + \frac{5}{8}\,\lambda^2\right)\sqrt{1+\lambda^2} + \frac{3}{8}\,\lambda^4 \ln \frac{1+\sqrt{1+\lambda^2}}{\lambda} \end{aligned}\right\} \cdots (16)$$

Numerical values for function $f_1(\lambda)$ are given in table I.

As second limiting case, we select the flight direction perpendicular to the propeller axis. Then,

$$v = (c^2 - 2c\, r\, \omega \cos\alpha + r^2\, \omega^2)^{1/2}$$

whereby α is the position angle of the peripheral direction relative to the flight direction. First we determine v^3 for one revolution; that is $\alpha = 0$ to 2π. This is accomplished with the aid of the defined integral:

$$\left.\begin{aligned} &\frac{1}{2\pi}\int_0^{2\pi} (1 - 2x\cos\alpha + x^2)^{3/2}\, d\alpha \\ &= 1 + \frac{5}{4}\,x^2 + \frac{9}{64}\,x^4 + \frac{1}{16}\,x^6 + \ldots \quad \text{for} \quad x < 1 \\ &= x^3 + \frac{5}{4}\,x + \frac{9}{64}\,x^{-1} + \frac{1}{16}\,x^{-3} + \ldots \quad \text{for} \quad x > 1 \end{aligned}\right\} \cdots (17)$$

obtainable by development of the integrand according to spherical functions.

Introducing (17) into (15) and posing $2l$ = constant and $\lambda \leq 1$, gives the friction power:

$$\left.\begin{aligned} N_R &= \rho\, u^3\, z\, l\, a\, \overline{c_w}\, f_2(\lambda) \\ &= \frac{\rho}{2}\, u^3\, F_{w_s}\, f_2(\lambda) \\ f_2(\lambda) &= \frac{1}{4} + \frac{5}{8}\,\lambda^2 + \lambda^4\left(\frac{5}{8} - \frac{9}{64}\ln\lambda\right) - \frac{1}{32}\,\lambda^6 - \ldots \end{aligned}\right\} \quad (18)$$

Numerical values of the $f_2(\lambda)$ function are given in table I. In the second case the friction power is consistently several percent lower than in the stationary case. Admittedly, our assumption of a constant mean value $\overline{c_w}$ is fairly rough. If we considered the actual flow on the inside parts of the blades, the friction power of the second case would be higher. Then the lowest possible friction power would probably be about the same in both cases. Again, it is natural to generalize these two results representing extreme cases to include any flight direction of the helicopter propeller. We assume that by proper control and blade twist the friction power is independent of the direction of flow. To compute the power the approximate assumption

$$f(\lambda) \sim \frac{1}{4} + \lambda^2 \tag{19}$$

valid for $\lambda \leq 0.6$ suffices in most cases.

TABLE I

λ	$f_1(\lambda)$	$f_2(\lambda)$	$f(\lambda)$
0	0.250	0.250	0.250
.1	.258	.256	.260
.2	.282	.276	.290
.3	.325	.313	.340
.4	.393	.369	.410
.5	.489	.451	.500
.6	.616	.564	.610
.7	.783	.714	
.8	.994	.909	
.9	1.253	1.155	
1.0	1.569	1.458	

When summing up the foregoing results, we can expect that the properly designed propeller in yaw is favorable both as regards the air mass engaged in producing the impulse and the friction power, and therefore constitutes a suitable and economical means for impulse creation.

Through the two foregoing assumptions, the impulse power and the friction power of the helicopter propeller have become independent of the direction of flow, thus making it possible to compute the power required for level

flight of this propeller approximately independent of the direction of flight. If F_w denotes the equivalent flat-plate area of the airplane fuselage, the total power required for sustained flight for the impulse force A is, according to (12), (18), and (19):

$$N = \frac{A^2}{2\rho F_s c} + \frac{\rho}{2} F_{w_s} \left(\frac{u^3}{4} + u c^2 \right) + \frac{\rho}{2} F_w c^3$$

Assuming the tip speed u = constant, we obtain the minimum of N by derivation, according to c and equating to zero:

$$\frac{dN}{dc} = - \frac{A^2}{2\rho F_s c_o^2} + \rho F_{w_s} u c_o + \frac{3}{2} \rho F_w c_o^2 = 0 \qquad (20)$$

The optimum value c_o of the rate of flow is readily computable from (20). From (12) follows:

$$w = \frac{A}{2\rho F_s c_o}$$

Now we assume the drag of the helicopter to be low and the impulse acting against the gravity. Then $A \sim G$. If the speed of climb v_z of the helicopter is given, the optimum angle of climb, according to figure 6, is:

$$\tan \varphi_o = \frac{v_z}{\sqrt{c_o^2 - (v_z + w)^2}} \qquad (21)$$

Equation (21) is applicable only when $v_z < c_o - w$, that is, for a helicopter with small excess of power. In this case, a diagonal climb with $\varphi_o < 90^\circ$ gives the highest speed of climb. But, if $v_z > c_o - w$, a case not realized as yet with existing helicopters, the vertical climb of $\varphi = 90^\circ$ is the best.

As the airplane body of the helicopter usually presents its smallest equivalent flat-plate area in the horizontal direction, the optimum climbing angle tends toward lower values than are to be expected according to equation (21).

As an illustrative example, let us study a helicopter with the following characteristics:

$G = 490$ kg $\qquad F_s = 14.40$ m^2

$\rho = .12 \frac{kg.s^2}{m^4}$ $\qquad F_{w_s} = .03$ m^2

$u = 130$ m/s $\qquad F_w = .10$ m^2

We obtain from (20):

$$c_o = 39.0 \text{ m/s} \qquad w = 3.63 \text{ m/s}$$

Even if stipulating the fairly high climbing speed of $v_z = 15$ m/s from this helicopter, the best climbing angle amounts to only $\varphi_o = 23.6^\circ$, according to equation (21).

So, as regards climbing flight, the conditions for the helicopter are very nearly those of the conventional airplane. By given power the greatest climbing speed is practically in no case reached by vertical ascent, as a superficial analysis of the helicopter might probably lead one to expect. Vertical ascent and hovering are quite uneconomical operating conditions of the helicopter and require a comparatively high specific horsepower. This maximum power is, however, presumably necessary only for a short period at take-off and landing. The airplane itself develops its maximum power mostly at take-off only.

The total propeller power can always be divided into the power N_s absorbed by the drive of the helicopter rotor and the power $v\,W$ absorbed by the drag of the whole helicopter rotor in flight direction. It is

$$N = N_s + v\,W$$

Now, there are two important limiting cases of horizontal flight:

1) Autogiro with auxiliary propeller: The autorotating propeller is driven only by its drag W through a special tractor propeller in the nose of the fuselage. At high speed - that is, for high values of λ, the propeller axis is almost exactly perpendicular to the flight direction, since only a very small angle of attack of the propeller-disk area acting as wing surface, is needed for impulse generation. Then there is the hazard of propeller failure, which may result in a crash.

This type of motive power is subject to considerable losses. At best the efficiency of the small tractor propeller is 0.70. Besides, vortex losses by the partial conversion of drag W of the propeller in a torque are to be expected.

2) Helicopter without auxiliary propeller: The propeller, driven solely by the initiation of a torque in the thrust axis, must therefore in horizontal flight yield in addition a traction in flight direction for overcoming the frictional drag of the airplane body. The angle between thrust axis and flight direction must in consequence be $\varphi < 90^\circ$ - that is, so much smaller as λ is greater. The danger of propeller failure does not exist. Contrasted with the autogiro the weight, friction power, and the higher power loss of impulse of the tractor propeller is saved. If the forward tilt of the rotor axis for a large enough angle and the balancing of the torque of the helicopter propeller can be solved constructionally, the second case of horizontal flight is preferable. Longitudinal stability is readily obtainable in this flight condition by conventional horizontal controls even for helicopters unstable when hovering. The Bréguet-Dorand helicopter developed in this manner a horizontal speed of 100 kilometers per hour in test flights held in December 1935 (reference 6).

The preliminary calculation of flight performances of helicopters fails at the present time for lack of sufficiently diversified six-component measurements on helicopters. This lack is also apparent in the stability calculation of the helicopter.

V. STABILITY OF THE HELICOPTER

Everyone is familiar with the toys consisting of a small propeller which is thrown in the air with a helical motion. Given enough ~~helix~~ angular momentum, these miniature helicopters are entirely stable. And still the technical solution of the stability problem of the helicopter has presented the greatest of all difficulties. The majority of helicopter projects heretofore have been wrecked by this very problem.

Apparently the stability makes a certain ~~free helix~~ of the helicopter a necessity. On the other hand, the floating of a person at one place requires a balancing of the torque of the helicopter rotor, which in most cases

was effected by pairs of propellers running in opposite directions. If, as frequently done, the two oppositely rotating propellers are of the same size, their ~~helix~~ becomes neutralized, thus leaving no free helical motion for the stabilization. The alternative, to make these propellers of different size, produces as a rule not enough free helical motion for stabilization unless other precautions are taken. Up to a few years ago, even six-component measurements of propellers in yaw were entirely nonexistent in literature, although they are indispensable for the theoretical study of the stability and for computing the necessary amount of free helical motion.

Curious to relate, this lasted for some time - until it occurred to someone to obtain the stability of the helicopter by mounting a control surface in the slipstream as suggested by the example of the airplane. The first designer to pursue this idea successfully by mounting the control surfaces sufficiently distant below a comparatively heavily loaded propeller, was O. Asboth. His designs, developed from 1928 to 1930, seem to have been the first man-carrying helicopters to hover for some time and at considerable height with perfect stability.

How does the stability of the helicopter with rigid propeller and control surfaces come about?

Assume that the helicopter is stable against vertical motions, and executing small motions only in the horizontal xy plane. The propeller center P may move toward P' with the coordinates $x_1 y_1$, the center of gravity S toward S' with the coordinates $x_2 y_2$, (fig. 7).

$$\alpha = \frac{x_2 - x_1}{h}, \qquad \beta = \frac{y_2 - y_1}{h}$$

are to represent the angles between the z-axis and the projections of the thrust axis on the xz plane and the yz plane.

Limiting the study to small equilibrium disturbances, we may assume in first approximation that the thrust is

$$K_a = mg = \text{constant}$$

and that the other aerodynamic loads and moments are proportional to the interference velocities $\dot{x}_1$ and $\dot{y}_1$. On the premises of small interference velocity Δv, we ob-

tain for the normal force acting against the direction of motion:

$$K_n = \zeta_n K_a \frac{\Delta v}{u}$$

for the lateral force acting at right angles to it:

$$K_s = \zeta_s K_a \frac{\Delta v}{u}$$

for the yawing moment acting in the plane rotor axis direction of motion:

$$M_h = \zeta_h K_a a \frac{\Delta v}{u}$$

and for the yawing moment acting at right angles to it:

$$M_r = \zeta_r K_a a \frac{\Delta v}{u}$$

The nondimensional ζ coefficients appended in table II are those for two propellers, according to Flachsbart's measurements (reference 7); λ_o is the axial coefficient of advance at which the thrust disappears. It serves to mark the propeller pitch. It will be seen that the ζ coefficients with the exception of ζ_r, appear to be little dependent on the propeller form.

TABLE II. Air Load and Moment Coefficients of Two Propellers

λ_o	ζ_n	ζ_s	ζ_h	ζ_r
0.10	0.27	0.12	1.08	0.77
.23	.30	.13	1.00	.43

We further make the simplifying assumption that the control surface is a coaxial ring so disposed that its center of pressure coincides with the center of gravity S of the helicopter (fig. 7). The control surface could, of course, be mounted at some other place, and if necessary, could consist of a flat surface, since the motions are coupled perpendicular and parallel to the surface through the precession moments. The motion resistance of the coaxial control surface lying in the slipstream is:

$$W = \frac{\rho}{2} w F c_a' \Delta v = p F \Delta v$$

that is, it is linearly dependent on the interference velocity, like the lift of an airplane wing. The control surface therefore affords, within certain limits, a stabilization.

The positive direction of rotation of the propeller is to correspond with the peripheral direction from + x-axis toward the + y-axis (fig. 7). Then the turning of the thrust axis produces the precession moments:

$$P_{yz} = J \omega \dot{\alpha}; \quad P_{xz} = J \omega \dot{\beta}$$

Expressing the angular changes and interference velocities by the coordinates x_1, y_1, x_2, y_2 and their derivations in time rate, we finally obtain for the equilibrium of the forces and the moments referred to center P the following equations:

$$\left.\begin{aligned}
&m \ddot{x}_2 + p F \dot{x}_2 + \zeta_n \frac{K_a}{u} \dot{x}_1 + \zeta_s \frac{K_a}{u} \dot{y}_1 \\
&\qquad + (x_2 - x_1) \frac{K_a}{h} = 0 \\
&m \ddot{y}_2 + p F \dot{y}_2 + \zeta_s \frac{K_a}{u} \dot{x}_1 + \zeta_n \frac{K_a}{u} \dot{y}_1 \\
&\qquad + (y_2 - y_1) \frac{K_a}{h} = 0 \\
&- \theta (\ddot{x}_2 - \ddot{x}_1) - p F h \dot{x}_2 + \zeta_h \frac{K_a}{\omega} \dot{x}_1 \\
&\qquad + \zeta_r \frac{K_a}{\omega} \dot{y}_1 + \frac{J\omega}{h} (\dot{y}_2 - \dot{y}_1) = 0 \\
&- \theta (\ddot{y}_2 - \ddot{y}_1) - p F h \dot{y}_2 + \zeta_r \frac{K_a}{\omega} \dot{x}_1 \\
&\qquad + \zeta_h \frac{K_a}{\omega} \dot{y}_1 + \frac{J\omega}{h} (\dot{x}_2 - \dot{x}_1) = 0
\end{aligned}\right\} \quad \cdots (22)$$

This system of linear differential equations are resolved by the known formulas:

$$\left.\begin{aligned} x_1 &= A\ e^{rt}, \quad & y_1 &= C\ e^{rt} \\ x_2 &= B\ e^{rt}, \quad & y_2 &= D\ e^{rt} \end{aligned}\right\} \quad \ldots\ldots \quad (23)$$

which, written in (22) finally give four homogeneous linear equations for the constants A, B, C, and D. These constants have no final values unless the denominator determinant of this system of equations disappears.

Writing, for abbreviation:

$$\left.\begin{aligned} a_1 &= \zeta_n \frac{Ka}{u} r - \frac{Ka}{h}, \quad & b_1 &= \frac{Ka}{h} + p F r + m r^2 \\ a_2 &= \zeta_s \frac{Ka}{u} r, & b_2 &= 0 \\ a_3 &= \zeta_h \frac{Ka}{\omega} r + \theta r^2, & b_3 &= - p F h r - \theta r^2 \\ a_4 &= \zeta_r \frac{Ka}{\omega} r - \frac{J\omega}{h} r, & b_4 &= \frac{J\omega}{h} r \end{aligned}\right\} \quad \ldots \quad (24)$$

The denominator determinant takes the following form:

$$\left.\begin{aligned} \Delta = \begin{vmatrix} a_1 & b_1 & a_2 & b_2 \\ a_2 & b_2 & a_1 & b_1 \\ a_3 & b_3 & a_4 & b_4 \\ a_4 & b_4 & a_3 & b_3 \end{vmatrix} &= -2 \begin{vmatrix} a_1 & b_1 \\ a_2 & b_2 \end{vmatrix} \cdot \begin{vmatrix} a_3 & b_3 \\ a_4 & b_4 \end{vmatrix} \\ - \begin{vmatrix} a_1 & b_1 \\ a_3 & b_3 \end{vmatrix}^2 + \begin{vmatrix} a_1 & b_1 \\ a_4 & b_4 \end{vmatrix}^2 &+ \begin{vmatrix} a_2 & b_2 \\ a_3 & b_3 \end{vmatrix}^2 - \begin{vmatrix} a_2 & b_2 \\ a_4 & b_4 \end{vmatrix}^2 \end{aligned}\right\} \quad \ldots \quad (25)$$

The lateral force K_s being, as a rule, small relative to the other forces, a_2 may be approximately put at $a_2 = 0$. In fact, this is exactly correct for oppositely rotating propellers, for which the lateral forces cancel out. In addition, $b_2 = 0$. Then the corresponding subdeterminants of equation (25) disappear, and the remaining equation $\Delta = 0$ may be divided into two equations, of which, however, only one has a physical sense. This reads:

$$- a_1 b_3 + a_3 b_1 + a_1 b_4 - a_4 b_1 = 0 \qquad (26)$$

Writing the values of equation (24) into (26) and arranging according to the powers of r, leaves, after segregating the minor root, $r = 0$:

$$\left.\begin{aligned} r^3 + r^2 \left[\zeta_n \frac{K_a}{mu} + \frac{pF}{m} + (\zeta_h - \zeta_r) \frac{K_a}{\omega\theta} + \frac{J\omega}{\theta h}\right] \\ + r \left[\frac{J\omega}{h\theta}\left(\zeta_n \frac{K_a}{mu} + \frac{pF}{m}\right)\right. \\ \left. + \frac{pF}{m}\left(\zeta_n \frac{hK_a}{u\theta} + (\zeta_h - \zeta_r) \frac{K_a}{\omega\theta}\right)\right] \\ - \frac{K_a}{\theta} \frac{pF}{m} + \frac{K_a}{hm} (\zeta_h - \zeta_r) \frac{K_a}{\omega\theta} = 0 \end{aligned}\right\} \cdots (27)$$

Stability exists when only roots r with negative real parts occur. This is with an equation of the form of

$$r^3 + a\, r^2 + b\, r + c = 0$$

the case only then, according to Hurwitz, when all coefficients are positive and when, in addition:

$$a\, b - c > 0 \qquad (28)$$

Since a and b are always positive, according to equation (27), it is only necessary to observe that:

$$c > 0 \qquad (29)$$

Equations (28) and (29) are therefore the desired stability conditions. Special importance attaches to the stability limits which are reached when putting either $ab - c = 0$ or $c = 0$. Then these equations should be used only for computing the requisite control surface or the required helical motion. The numerical calculation can be simplified by neglecting small terms, after which the equations for the control surface from (28) and (29) read:

$$\left.\begin{aligned} &\text{I.} \quad F \geq \frac{1}{p} \frac{\gamma\, e_2\, e_6 - \kappa\, e_1\, e_4 (e_1 + \gamma\, e_2 + \kappa\, e_4)}{e_5 + \kappa (e_1 - e_3)\, e_4 + (e_1 + \gamma\, e_2 + \kappa\, e_4)^2} \\ &\text{II.} \quad F \leq \frac{\gamma}{p} \frac{e_2\, e_6}{e_5} \end{aligned}\right\} \cdots\cdots (30)$$

The abbreviations hereby are:

$$\left.\begin{aligned} e_1 &= \zeta_n \frac{K_a}{mu}, & \kappa\, e_4 &= \frac{J\omega}{h\theta} \\ \gamma\, e_2 &= (\zeta_h - \zeta_r) \frac{K_a}{\omega\theta}, & e_5 &= \frac{K_a}{\theta} \\ e_3 &= \zeta_n \frac{hK_a}{\theta u}, & e_6 &= \frac{K_a}{hm} \end{aligned}\right\} \quad \ldots\ldots \quad (31)$$

The factors γ and κ are nondimensional criteria for the difference of yawing moment and rolling moment and for the free helical motion of the helicopter propellers. At $\gamma = 1$ the rolling moment $M_r = 0$ at $\kappa = 1$, the free helical motion equals the helix of a certain helicopter problem.

The following is an illustrative example, patterned somewhat after the Asboth helicopter. This helicopter has two coaxial rotors running in opposite directions, rigid blades, and is characterized by small dimensions. We put:

$a = 2.14$ m	$N = 100$ hp.	$\zeta_n = 0.30$
$h = 1.0$ m	$w = 20$ m/s	$\zeta_h = 1.00$
$k = 1.0$ m	$u = 130$ m/s	$\zeta_r = .50$
$G = 490$ kg	$J = 10$ m kg s^2	$c_a' = 4.0$

$h\theta = 100$ m kg s^2

and obtain for the control surface as function of κ and γ the values plotted in figure 8. Having to observe two stability criteria, the size of the control surface must not fall below a minimum value nor exceed a maximum if stability is to be maintained. Figure 8, therefore, shows the stability range by predetermined γ bounded by two lines, which start almost from the same point of the ordinate axis. At $\kappa = 0$, that is, propeller entirely free from helical motion, the stability range shrinks almost to zero. In this case, even a control surface can at best assure only neutral stability.

In practice, however, a certain amount of residual helix of the oppositely rotating propellers will always be available. Then a suitably dimensioned control surface will give stability. Assuming for Asboth's helicopter a 20-percent difference in helix, that is $\kappa = 0.2$ and

$\gamma = 1.0$, figure 8 gives as possible control surface $F = 1.13$ to $1.61\ m^2$, which amounts to about 10 percent of the rotor disk area. Its actual control surface is probably of the same order of magnitude. The permissible range in control surface size becomes so much larger as κ is higher; i.e., as the helix is greater. Once the helix reaches a certain value ($\kappa = 0.7$ at $\gamma = 0.5$ in fig. 8), stability may be attained even without control surface.

To render the curves intelligible, we also plotted in figure 8, negative values of F at higher values of κ, which, however, have no physical significance.

The greater the rolling moment, i.e., the smaller γ is, that much less is the required helix or the necessary control surface. In other words, the rolling moment has a stabilizing effect. Unfortunately, it is impossible, in practice, to raise the rolling moment beyond a certain amount. It can even disappear altogether for oppositely running propellers if they are of the same size and speed.

How great must the helical motion of a helicopter be to be stable without control surface? Obviously, then, when the numerator in (30)I disappears. Neglecting progressively $e_1 + \gamma e_2$ with respect to κe_4, the introduction of (31) gives as stability condition of the single rotor-helicopter

$$J > \frac{1}{u}\sqrt{\frac{\zeta_h - \zeta_r}{\zeta_n} G a^3 \theta h}$$

or, using the figures of our example:

$$J > \frac{1}{130}\sqrt{\frac{0.5}{0.3} 450 \times 2.14^3 \times 100} = 6.58\ m\ kg\ s^2$$

For a radius of inertia of ~ 0.55 a, this inertia moment would correspond to a rotor weight of at least 50 kilograms. It consequently requires a fairly enormous inertia moment for stabilization without control surface. The conditions become a little more favorable as a result of the greater diameter on a lightly loaded autogiro rotor. We assume for this:

$$a = 4.9\ m \qquad \zeta_n = 0.27$$

$$\zeta_h = 1.08$$

$$\zeta_r = .77$$

the other values to remain as before. Then the moment of inertia becomes:

$$J > \frac{1}{130}\sqrt{\frac{0.31}{0.27} \times 490 \times 4.9^3 \times 100} = 19.8 \text{ m kg s}^2$$

This corresponds to a rotor weight of at least 28 kilograms. The actual rotor of a corresponding autogiro is somewhat lighter, so that it would fall short for stabilization, even with fixed blades. Substantially more unfavorable is the case of oppositely rotating rotors. Then, $\zeta_r = 0$,

$$J > 37.0 \text{ m kg s}^2$$

This helix could be assured by lodging a balance weight of about 15 kilograms in the blade tips of a rotor.

The majority of the newer helicopters have lightly loaded rotors with small articulated blades, on the order of the autogiro. Every blade hinge introduces a new degree of freedom. The flexural flexibility of the small blades has, in principle, a similar effect. This renders the theoretical investigation of the stability extraordinarily difficult.

Even the autogiro, with its known light rotor, becomes unstable at low flying speed, but the oscillation period is so great that controlled stability is possible, at which the pilot corrects the yawing motions by appropriate control deflections. All helicopters having two opposingly running rotors of this kind are known to be even less stable when hovering. If the oscillation period is long enough a skilled pilot is, however, as a rule, able to rise approximately vertically and to hover for a short time, so as to attain the horizontal speed as soon as possible, where the relative wind and horizontal control establish longitudinal stability.

Controlled stabilization is facilitated in a certain respect if the two oppositely rotating rotors are side by side. Then the pilot needs only to control the rotation about the line connecting both rotors, because the rotation about the axis perpendicular to it is largely damped by the opposingly directed lift change of the two rotors. Controlled stabilization with two coaxial rotors is probably much more difficult. Then it does not involve the complete solution of the helicopter problem but rather another transition stage from autogiro to helicopter.

The captive helicopter has always claimed a certain amount of interest in regard to its applicability to military, meteorological, and radiotelegraphic purposes. The first man-carrying captive helicopter was built in Austria in 1918 (reference 9). It had two coaxial propellers running in opposite directions, and was raised and lowered by three cables and winches. The helicopter then has the static stability of the three-point support. Mooring a helicopter by one cable only would remove the principle of the dynamic stability, namely, the constant direction of the extraneous force applied at the center of gravity. Then the gravity could combine itself with the cable force into a resultant - to a certain extent - in any direction. This case has been elaborated by von Kármán (reference 10).

It is, to be sure, conceivable that controlled stability can be attained in this case also, whereby the helicopter executes certain pendulous motions of moderate size, such as occur on captive balloons by wind changes. The pilot might be relieved of this control labor by proper instruments which respond to inclinations of the aircraft with respect to an artificial horizon or to rotary accelerations, such as already have attained to a certain stage of development for the automatic control of the conventional airplane. Stability in free flight is probably a necessary requisite for the controlled stabilization of a helicopter moored by a cable.

VI. HELICOPTER DRIVE

One of the most difficult problems in helicopter design is the drive of the rotor without reaction on the airplane body. Owing to its naturally large rotor diameter, the torque itself is unusually high compared to the usual airplane power plants. Its gears must therefore also be comparatively large. Added to this, the necessity of torque balance to assure hovering without rotation of the airplane body - it is not surprising that a series of clumsy helicopter designs made their appearance which up to now have caused the professional airplane designer to steer clear of the subject. The energies of the designer were exhausted on the drive problem, so that the stability problem generally received no adequate treatment. The results were not very satisfactory, and it was these very difficulties that decided de la Cierva to make an autogiro

driven by air speed out of the helicopter propeller driven by turning moments.

A brief summary of the constructive means resorted to heretofore to balance the torque (turning moment) may be of interest.

Most builders of helicopters obtained this balance by resorting to rotors in pairs, driven by initiation of turning moments in the thrust axis. The most important arrangements in this category are:

1. Coaxial, oppositely rotating, 16 types.

2. Side by side, with parallel axes, oppositely rotating, 9 types.

3. Side by side, with tilted axes, rotating in the same direction, 2 types.

A single rotor is sufficient if the balance of its turning moment is effected by auxiliary propellers with horizontal axes. The possible arrangements are:

4. Auxiliary propellers on body, 2 types.

5. Auxiliary propellers on the rotor blades, 4 design types.

This list is essentially that of Lamé (reference 1), brought up to date as much as possible. Constructionally clearest and consequently most popular is arrangement 1. Successful designers of this type are Asboth, D'Ascanio, and Breguet-Dorand. Next in popularity came Oemichen's "helicopter of the first kilometer," in category 2. The advantage of this class lies in the smaller, higher-speed rotors, and in its more easily attainable controlled stability than with arrangement 1. Its objectionable features are the bulky booms on which the rotors are mounted.

Quite recently Platt (reference 11) investigated a limiting case of arrangement 1: The "countervane" attains a considerably greater area and does not turn but is rigidly mounted to the airplane. For a disk area loading of $\frac{A}{F_s} \sim 10$ kg/m^2, as found on modern autogiros and helicopters, the fairly large surface $F \sim 0.2\ F_s$ is necessary, and is located parallel to the direction of flight. This

arrangement should be little suited for high-speed flight. For $s > a$ the effect of the ground on the moment balance is insignificant.

Particular interest attaches to Florine's arrangement, 3, which may be called partly birotatory, because the two rotor axes are set obliquely to produce through the horizontal component of the rotor thrust a couple balancing the driving moments of the two rotors. The free helical motion of the rotors is only partly neutralized, leaving a large remainder for stabilization.

Inasmuch as acceptable horizontal speeds as well as autorotation of rotors in case of engine failure, are expected from a modern helicopter, arrangements 4 and 5 are probably ruled out in the future development of free-flying helicopters. In point of fact, comparatively few have ever been built on account of the enormous constructional difficulties. To be sure, the possibility of needing only one rotor is so tempting that Glauert considered arrangement 5 as "the most promising form of energy transmission to the blades of a rotor" (reference 12).

Let us see if this ideal - that is, the helicopter with a single rotor - is not attainable in some other way. The most frequently built coaxial, oppositely rotating rotor pair comprises two rotors whose angular velocity vectors differ by $2\delta = 180^\circ$ in the direction. With articulated blades this angle changes in turning. Unless the two rotor hubs are far enough apart, there is danger of collision of the oppositely rotating blades when making a turn. This distance must in any case be greater than 10 percent of the rotor diameter as experience has demonstrated with the Bréguet-Dorand helicopter. This results in an undesirably high location of the upper rotor hub. There is also an absence of the free helical motion needed for stability, if $2\delta = 180^\circ$. Now, however, arrangement 3 shows that moment balancing is equally attainable with comparatively small δ; that is to say, partly contrarotation.

For articulated blades, the vector of the angular velocity can, by proper periodical motion of the blade hinge, very well form an angle with the "metallic" propeller axis. Modern design types generally make use of this fact for the servo control of helicopters. So, if we utilize a control of this kind, we can visualize two rotors rotating oppositely at an angle of 2δ as being combined on one hub,

wherein the blades of the first rotor revolve between the blades of the second rotor.

For simplicity, we assume each propeller as consisting of one blade only. The two blades of the two propellers, cased in one another, are disposed diametrically. Then the blade axes vary their angle relative to the metallic propeller axis periodically; that is, by $\pm\vartheta$. Assuming the described blade motion to be positive, we can, on the other hand, produce a periodic moment about the blade hinge by means of periodical blade-angle control. If this moment is in phase with the periodic change of angle, we can transmit power on our propeller by means of the hinge. Having two diametral blades, the two hinge moments neutralize each other without causing a reaction on the propeller axis or the airplane body. Only the rotor blade is stressed in bending. By varying angle ϑ, of blade-bending moment and phase angle, we can regulate the transmitted power at will within certain limits and fit it to the amount needed to produce the thrust. We have, in fact, a partially oppositely rotating propeller arrangement with only one hub and only one metallic propeller axis, which induces no torque reaction on the airplane body.

The basic idea of this type of drive was published by Passat in 1921 (reference 13), and merits recall from oblivion. Passat built a helicopter model with one rotor, having four "bird-shaped" blades, which flap and rotate. A lift of 90 kilograms with 10 horsepower was claimed for it. Further details are unknown to the writer. The blades probably rotated about their hinge axes, so that $\vartheta = B$. In that case, only a comparatively little power can be transmitted because the angular amplitude B is limited to about 10° as a result of the burbling of the flow at the blade profiles.

Each pair of diametral blades produces, during up-and-down flapping, a periodical, axially directed mass (or inertia) force, conformable to its own mass. In order to neutralize this disturbing mass force, which would shake the airplane body, we must have another mass going through a similar but opposite motion. This might be a second pair of blades disposed in peripheral direction, thus giving us a four-blade rotor. However, this is not fundamentally necessary. The essential factor is the paired diametral blade arrangement.

It should perhaps be added that one frequently finds in patent literature an arrangement whereby the rotor as a whole executes an oscillating motion in axial direction. From the aerodynamic point of view, this method can also be used to transmit flapping power. The balancing of the mass forces would require two oppositely swinging rotor hubs, through which the unity of the rotor is lost again. Aside from that, the bending moments in the rotor blades caused by the mass forces make the constructional execution of such full-size rotors impossible. For that reason, we shall take only the flapping drive of the above-mentioned method into consideration.

An observer, turning with the rotor axis, sees the blades make one up-and-down flapping motion during each revolution. We may therefore speak of a flapping drive of the blades, but with one provision. To an observer standing still, each blade appears to move in a certain plane; that is, on a conical surface by rotor-thrust loading. The movement of both blade axes therefore is altogether like the movement of two normal one-blade rotors so fitting into each other that they receive one common hub and are partly oppositely rotating.

The blades resist the deflection from their natural surface of motion energetically. In consequence, the flapping frequency cannot be raised at will in order to transmit as much power as possible, but is strictly bound to the rotation speed. Otherwise, the mass forces would set up a "blind moment" which would more than offset the "active motion," and so render the construction of a sufficiently strong rotor blade an impossibility.

In the following, this flapping drive of the rotor is analyzed theoretically.

Assume a rotor with one blade rotating in a plane E at constant speed $\omega = \nu$ (fig. 9), while at the same time this blade executes rotary oscillations about its neutral axis with the same circular frequency ν and the amplitude B. Assume further that the rate of flow through the rotor is negligibly small with respect to the tip speed. By means of the nonstationary airfoil theory, the moment of the rotor blade with respect to an assumed axis lying in the plane of motion and meeting the rotor axis at right angles, can be readily determined. Using the notation of Küssner from his report on nonstationary lift (reference 14), and assuming plane flow - a condition

closely met by the small rotor blades - the moment is:

$$M = \pi \rho v^2 B e^{i\nu t} \int_0^a \left[\left(1 + i \frac{l}{r}\right)\left(1 + T\left(\frac{l}{r}\right)\right) + i \frac{l}{r} - \frac{l^2}{2r^2} \right] l r^3 dr \qquad (32)$$

(T is a complex function tabulated in reference 14.) The evaluation of this integral calls for assumptions regarding the blade chord $2l$. We analyze three blade forms:

1. $l = 0.068\ a - 0.050\ r$

2. $l = .030\ a$

3. $l = .050\ a$

The blade tips are half round.

As $\nu = \omega$, according to assumption, the moment at the blade hinge is:

$$M = \rho u^2 F_s a B m e^{i\nu t} \quad m\ kg \qquad (33)$$

The complex moment coefficient m is obtained by graphical integration and shown in table III for the three blade forms; m' and m" denote the real and the imaginary parts; $\bar{m}$ the absolute amount of this coefficient.

The periodic circulation variation of the blade produces a vortex loss which is also computable according to Küssner (reference 14). In that manner a resisting moment about the axis of rotation D is created; its mean loss of power is:

$$\left.\begin{aligned} H_m &= \frac{1}{4} \pi \rho \nu^2 B^2 \int_0^a \left[1 - \bar{T}^2 \left(\frac{l}{r}\right)\right]\left[1 + \frac{l^2}{r^2}\right] l r^3 dr \\ &= \rho u^3 F_s B^2 h \quad m\ kg\ s \end{aligned}\right\} \cdots (34)$$

The real coefficient h is given in table III for the three blade forms.

TABLE III. Coefficients of the Flapping Drive

Blade form	Moment coefficients			Drag coefficients	
	m'	m''	$\bar{m}$	h	h_r
1	0.0128	0.0020	0.0130	0.000417	0.00221
2	.0140	.0025	.0142	.000394	.00233
3	.0214	.0045	.0218	.000992	.00381

The choice of form and curvature of a blade section is, as a rule, for smallest possible frictional drag of the section by a given lift coefficient, which corresponds to an angle of incidence for the most frequent running condition. For small angular variations the drag coefficient is approximated by means of the power series:

$$c_w = \sum_0^\infty c_{w_n} (\beta - \beta_0)^n$$

Posing $\beta - \beta_0 = B\, e^{i\nu t}$, the entire mean friction power of the blade with assumedly constant profile, becomes:

$$H_r = \rho\, \nu^3 \int_0^a l\, r^3\, dr \left[c_{w_0} + \frac{1}{2} c_{w_2} B^2 + \frac{3}{8} c_{w_4} B^4 + \ldots \right]$$

The first term of this equation represents the inevitable friction loss produced by stationary flow and already contained in equation (16). The other terms must be ascribed to the flapping drive. We write for the friction loss:

$$H_r = \rho\, u^3\, F_s\, h_r \left[c_{w_0} + \frac{1}{2} c_{w_2} B^2 + \frac{3}{8} c_{w_4} B^4 + \ldots \right] \quad (35)$$

The coefficient h_r is also included in table III. The departures from the stationary flow of the analyzed blade forms amount to a few percent only. Therefore the friction loss H_r exceeds the vortex loss H_m substantially. The movement of the blade hinge being in a plane E with constant angular velocity, according to our assumption, the flapping angle is, according to figure 9:

$$\sin \gamma = \sin \vartheta \cos \nu\, t \quad (36)$$

The blade-bending moment M, whose axis of reference

in plane E lies perpendicular to the blade axis, can be divided into two components. The component transmitting flapping power must have a moment axis perpendicular to the rotor axis SS and therefore amounts to

$$M_s = M \frac{\cos \vartheta}{\cos \gamma} \tag{37}$$

If ϑ is the phase angle between the time period of the maximum bending moment of the first order of the blade and the passage of the blade axis through the position perpendicular to the rotor axis, the mean flapping power is, according to equations (32), (36), and (37):

$$\left.\begin{aligned} L &= \nu \cos \varphi \frac{1}{2\pi} \oint M_s \, d\gamma \\ &= \nu \cos \varphi \frac{1}{2\pi} \int_0^{2\pi/\nu} M \frac{\cos \vartheta}{\cos \gamma} \frac{d\gamma}{dt} \, dt \\ &= \rho u^3 F_s B \bar{m} \cos \varphi \sin \vartheta \cos \vartheta \\ &\qquad \frac{1}{2\pi} \int_0^{2\pi} \frac{\sin^2 \alpha}{1 - \sin^2 \vartheta \cos^2 \alpha} \, d\alpha \\ L &= \rho u^3 F_s B \bar{m} \cos \varphi \cos \vartheta \tan \frac{\vartheta}{2} \end{aligned}\right\} \quad \cdots \quad (38)$$

With given tip speed u the power losses are only dependent on the amplitude of rotation B of the blade, according to equations (33) and (35). In order to transmit as much flapping power L as possible by predetermined losses and thereby attain a high drive efficiency, the angles φ and ϑ must be chosen propitiously. It involves no difficulties to so control the blade angle β that the phase angle becomes $\varphi = 0$. Then $\cos \varphi = 1$. For given phase angle, the power becomes maximum if

$$\cos^3 \vartheta - 2 \cos \vartheta + 1 = 0$$

$$\cos \vartheta = 0.619; \quad \vartheta = 51^\circ 45'$$

Admittedly, this optimum angle of opposite rotation is excessively great. Besides, the constructive optimum lies at a smaller angle since the rotor is to produce a thrust in the direction of the "metallic" rotor axis SS

contrary to the force of gravity. If the motion planes of the rotor blades diverge materially from the normal plane to SS, the thrust coefficient may decrease. It may therefore be presumed that $\vartheta \sim 30^{\circ}$ is about the upper limit of the practically permissible angle of opposite rotation.

For the purpose of a comparative computation, let us assume that a blade requires a moment coefficient of

$$k_{d_o} = 0.00025$$

for impulse generation, which would approximately correspond to the thrust coefficient of

$$k_s = 0.0134$$

for a four-blade rotor in hovering condition.

Now, let us see how great the total rotor power required with flapping drive is, under this assumption, for our three particular blade forms.

The writer's own measurements on model rotors with Joukowski profiles of small thickness and curvature, gave the following drag coefficients:

$$\left.\begin{aligned} c_{w_o} &= 0.011 \\ c_{w_2} &= 1.1 \\ c_{w_4} &= 0 \end{aligned}\right\} \quad \text{for} \quad B \leq 0.15$$

In accord with the previous assumptions, we obtain from equations (34), (35), and (38) the moment coefficient on the one hand, as transmitted, and on the other hand, as absorbed power:

$$k_d = k_{d_o} + 2h\,B^2 + h_r\,(2c_{w_o} + c_{w_2}\,B^2) \tag{39}$$

$$k_d = 2\bar{m}\cos\vartheta\,\tan\frac{\vartheta}{2}\,B \tag{40}$$

Then the required antirotation angle and the moment coefficient k_d can be computed for different blade rotation amplitudes B from (39) and (40). The results are shown in table IV. The ratio $\epsilon = k_d/k_s$, is computed with a thrust proportion for one blade at

$$k_s' = \frac{1}{4} k_s = 3.35 \times 10^{-3}$$

If the previously made "sphere" assumption of the quantity of flow holds true, the thrust would have to be independent of the antirotation angle ϑ. In experiments - to be published later, in detail - the thrust remained practically constant within the test range $\vartheta = 0$ to 10°, according to which the efficiency of the flapping drive is:

$$\eta = \frac{k_{d_o} + 2c_{w_o} h_r}{k_d}$$

TABLE IV. Rotor Blade with Flapping Drive

No.	B	0.05	0.10	0.15
1	$k_d \times 10^3$	0.307	0.331	0.372
	η	.973	.901	.802
	ϵ	.092	.099	.111
	ϑ°	30.7	15.0	11.1
2	$k_d \times 10^3$	0.310	0.335	0.377
	η	.973	.900	.803
	ϵ	.092	.100	.113
	ϑ°	27.6	13.8	9.7
3	$k_d \times 10^3$	0.349	0.396	0.473
	η	.956	.843	.705
	ϵ	.104	.118	.141
	ϑ°	19.2	10.5	8.3

Unless the antirotation angle ϑ is too small, good rotor ϵ and good efficiencies of the flapping drive are obtainable, according to table IV - superior to the drive by autorotation in the relative wind. Moreover, it is desirable for mechanical reasons to keep the rotation amplitude B, which governs the losses, to a minimum in order to keep the flexural stresses of the rotor blades and consequently the structural weight, to a minimum. With regard to the separation of flow, it must be $B < 0.17$, corresponding to 10° in degrees of angle. In the full size this limit will, moreover, not be attainable for reasons of strength. At $\vartheta = 30^\circ$, the highest value of the periodic bending moment is of the same order of magnitude as

the bending moment of the rotor blade under stationary normal thrust load; that is, of controllable order of magnitude.

The decisive advantage of this flapping drive is the unity of the rotor, which assumes:

1) a compact helicopter design;

2) sufficient free helical motion for stabilization;

3) a low drag at high speed.

Danger that the rotor blades may flap simultaneously, does not exist. Aurotation is possible after stopping or failure of the flapping drive, since the blade form is not substantially different from that of the autogiro, and the blades are likewise hinged at the hub.

On the other hand, we must not forget its disadvantages. These are:

1) stronger and heavier rotor blades capable of withstanding the high bending stress are required;

2) additional losses because of the mechanical transmission of the flapping power from the engine to the blades.

The purpose of these expositions was to show that, from the aerodynamic point of view the flapping drive appears practical, and contains no secondary conditions which from the very beginning would militate against their being constructionally feasible.

The flapping drive of the rotor is a mechanical analogy to the electric alternating-current synchronous motor. The blade moment ωB corresponds to the amperage J and the angle of antirotation ϑ to the voltage E. The phase angle φ has the same significance in both cases. The loss $H_m \omega B^2$ corresponds to the copper loss ωJ^2; the loss H_r is comparable to the iron loss, since in neither case does a simple relation exist between B and J.

The rotor with pure flapping drive is just as little capable of starting by itself as is the electric synchronous motor. It is therefore proper to actuate the rotor shaft normally by initiating a torque and then effecting

the change into flapping power at the rotor shaft itself by wobble plates. Then starting presents no difficulty and more than that, one is in position to control the degree of equalization at will and to induce free positive or negative moments which allow the aircraft to turn in any desired direction while hovering.

Horizontal high-speed flight of the helicopter does not necessarily demand an absolutely moment-free rotor drive. It might be that in this case the balancing of the driving moment by a force couple is more economical; this is produced through the reactions of the relative wind at two suitably distant control surfaces. As is known, pursuit airplanes with very light power loading can climb vertically like a helicopter by neutralizing the propeller driving moment through aileron deflection; that is, through a couple at the wing tips.

VII. OUTLOOK

Heretofore the propeller has been almost exclusively known as a machine for creating a stationary thrust in axially symmetrical stationary flow. The discovery that, with suitable form and control of blades, it can also develop valuable qualities in other than axially symmetrical stationary flow - which, to be sure, are difficult to treat theoretically, although practically provable - has brought us considerably closer to the complete solution of the helicopter problem. In order to continue in this direction, these qualities of the rotor must be theoretically and experimentally explored and in the same detail as in respect to the axially symmetrical flow. For with the real helicopter we always have to count on departures from the axially symmetrical flow, whether in stability investigations or in computing flight performance or flapping drive.

Translation by J. Vanier,
National Advisory Committee
for Aeronautics.

REFERENCES

1. Lamé: Le vol vertical. Paris, 1934.
2. Luftwissen, Bd. 3 (1936), S. 215.
3. Kimmel, H.: Z.F.M., Bd. 3 (1912), S. 53.
4. Walchner, O.: Luftfahrtforschung, Bd. 13 (1936), S. 103.

4a. Schrenk, M.: Z.F.M., Bd. 24 (1933), S. 416.

5. Margoulis, M. W.: C. R. Acad. Sci., Paris, Bd. 198, (1934), S. 1474.
6. Flugsport, Bd. 28 (1936), S. 47 und 358.
7. Flachsbart, O., and Kröber, G.: Experimental Investigation of Aircraft Propellers Exposed to Oblique Air Currents. T.M. No. 562, N.A.C.A., 1930.
8. Jour. Roy. Aero. Soc., vol. 35 (1931), p. 630.
9. Z.F.M., Bd. 12 (1921), S. 357.
10. von Kármán, Th.; Z.F.M., Bd. 12 (1921), S. 352.
11. Platt, H. H.: The Helicopter: Propulsion and Torque. Jour. of the Aeronautical Sciences, vol. 3, no. 11, September 1936, p. 398.
12. Glauert, H.: On the Horizontal Flight of a Helicopter. R. & M. 1157, British A.R.C., 1928.
13. Flight, vol. 13 (1921), p. 277; Z.F.M., Bd. 12 (1921), S. 190.
14. Küssner, H. G.: Luftforschung, Bd. 13 (1936), S. 410.

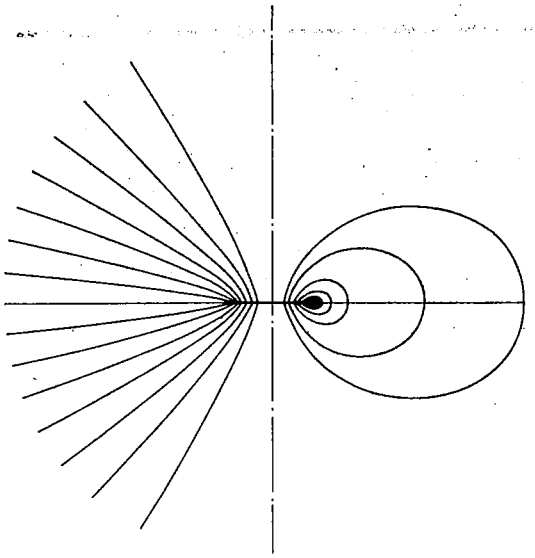

Figure 1.- Components of the airflow through the rotor disk area.

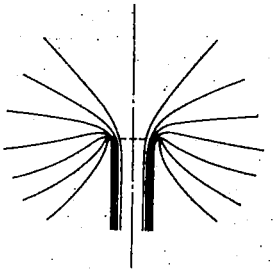

Figure 2.- Axially symmetrical ideal flow about a rotor.

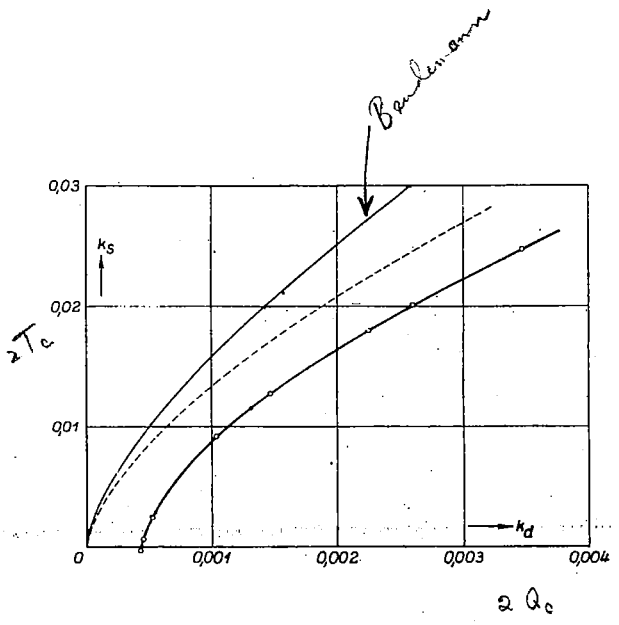

Figure 3.- Polar of a rotor.

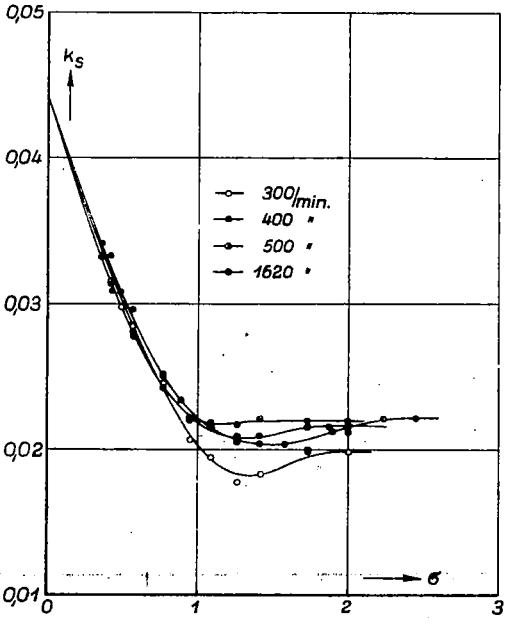

Figure 4.- Thrust coefficient of rotor at different wall distance.

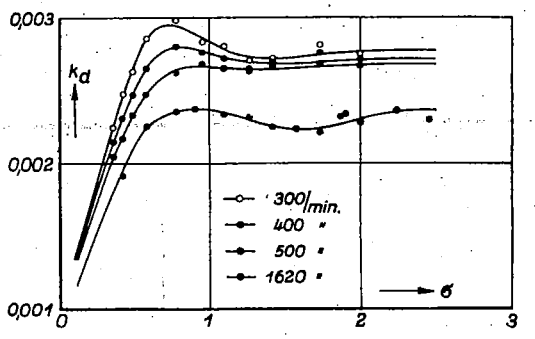

Figure 5.- Moment coefficient of rotor at different wall distance.

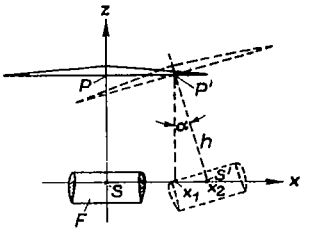

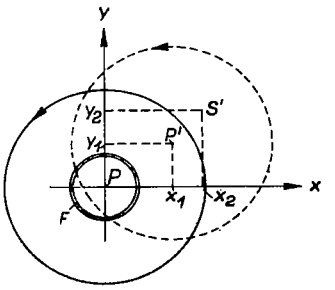

Figure 7.- Helicopter with control surface (diagrammetical).

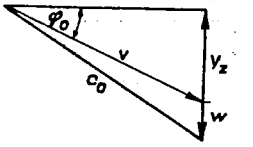

Figure 6.- Angle of climb.

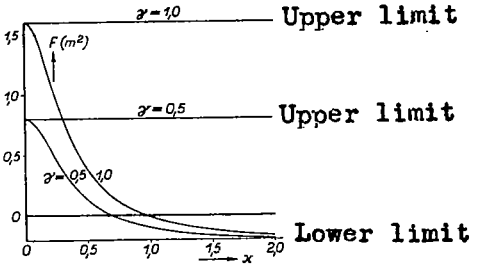

Figure 8.- Stability of the Asboth helicopter.

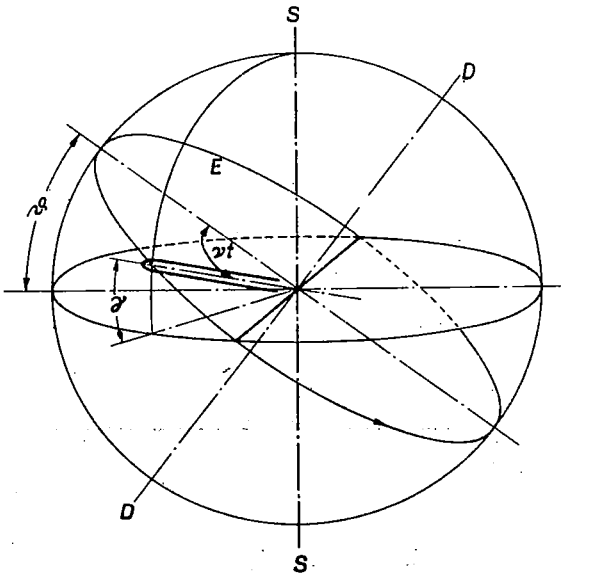

Figure 9.- Perspective drawing of rotor blade movement.